Final Technical Report for USGS NEHRP Award G17AP00029

3D Shear Velocity Structure in the Mendocino Triple Junction Region

Principal Investigator(s): Jeffrey Joseph McGuire
Dept. of Geology and Geophysics, WHOI
266 Woods Hole Rd.
Woods Hole MA, 02543

508-289-3290, jmcguire@whoi.edu

Proposed Start Date: January 1, 2017

Proposed End Date: December 31, 2017

Abstract

The southernmost ~200 km of the Cascadia subduction zone and incoming Gorda plate is one of the most seismically active regions of the United States, regularly generating magnitude > 6 earthquakes including the M7 Petrolia thrust event in 1992. This part of the Cascadia subduciton zone has the shortest average recurrence intervals of M8 earthquakes on the thrust interface at about 240 years [*Goldfinger et al.*, 2012] but it has been a difficult region to study because the locked zone occurs primarily offshore. Recently, the NSF Cascadia Initiative, combined with the Plate Boundary Observatory and the Northern California Seismic Network have collected a dense onshore-offshore seismic dataset that is unique for its ability to characterize the seismicity on and near the thrust interface. The existing structural models have proven to be insufficient for doing automated phase associations and earthquake locations well with this density of stations. We have built a new high-resolution (~3km) 3D P and S-wave seismic velocity model using the combined offshore and onshore datasets. The new velocity model shows the subduction of the Gorda plate down to about 30 km depth. It clarifies the location of the top of the oceanic crust relative to the Cascadia plate boundary model and it demnonstrates that the 1992 M7.2 Pretolia earthquake was not on the plate boundary. We have begun the process of using the new velocity model to refine the plate boundary model.

Final Report

The southernmost ~200 km or so of the Cascadia subduction zone is one of the most seismically active regions of the United States, regularly generating magnitude > 6 earthquakes (Figure 1) including a M7 thrust event in 1992 that likely occurred within the overriding plate [*Murray et al.*, 1996]. This part of the Cascadia subduciton zone has the shortest average recurrence intervals of M8 earthquakes on the thrust interface at about 240 years [*Goldfinger et al.*, 2012] and has been difficult to study because the locked zone occurs primarly offshore (Figure 1). Recently, the NSF funded Cascadia Initiative, combined with the Plate Boundary Observatory and Northern California Seismic Networks, collected a dense onshore-offshore seismic dataset that is unique for its ability to characterize the seismicity on and near the thrust interface (Figure 2). We have been working on this region using a combination of onshore and offshore seismic data [*Chen and McGuire*, 2016] as well as onshore geodetic data [*Wei and McGuire*, 2014] to understand the variations in fault strength and earthquake rupture dynamics between the different fault systems as part of a NSF funded project. In doing this work, it has become clear that to accurately study this region, a very high-resolution 3-dimensional shear-wave velocity model is required that covers both the onshore and offshore seismically active regions. Even from simple travel-time measurements it is clear that the offshore part of the overriding plate has a very high Vp/Vs ratio, likely indicating high-porosity in the accretionary wedge. We proposed to perform an update to both the Vp and Vs models within the MTJ region.

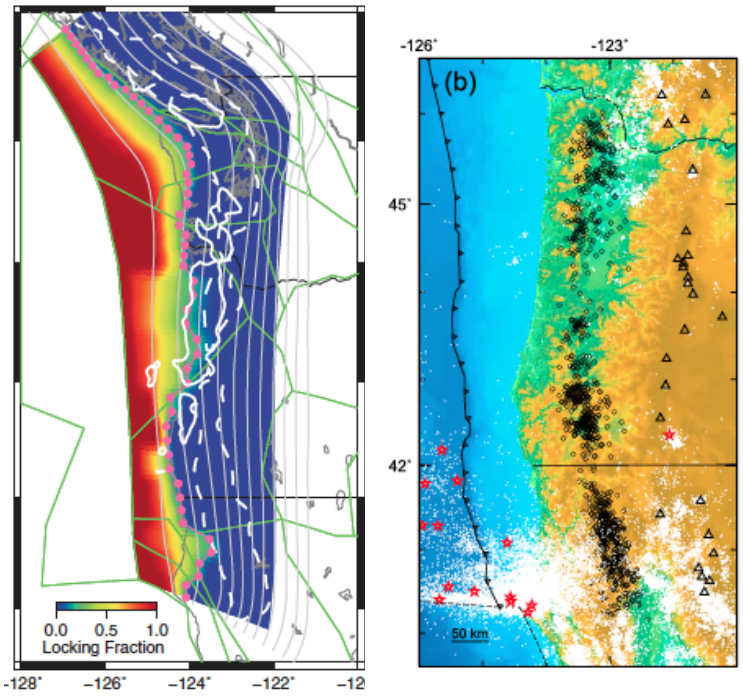

Figure 1. Left) From *Schmalzle et al.* [2014]. Colors show the interseismic locking distribution on the plate interface from a recent geodetic inversion. The solid white contours show the location of volcanic terrains identified from the gravity field. The dashed contours show the location of tremor epicenters along the length of Cascadia. Right) from *Boyarko and Brudzinski* [2010]. A map of southern Cascadia showing tremor locations (black circles) and seismicity (white dots) as well as the location of large earthquakes (red stars) in the subducting Gorda plate.

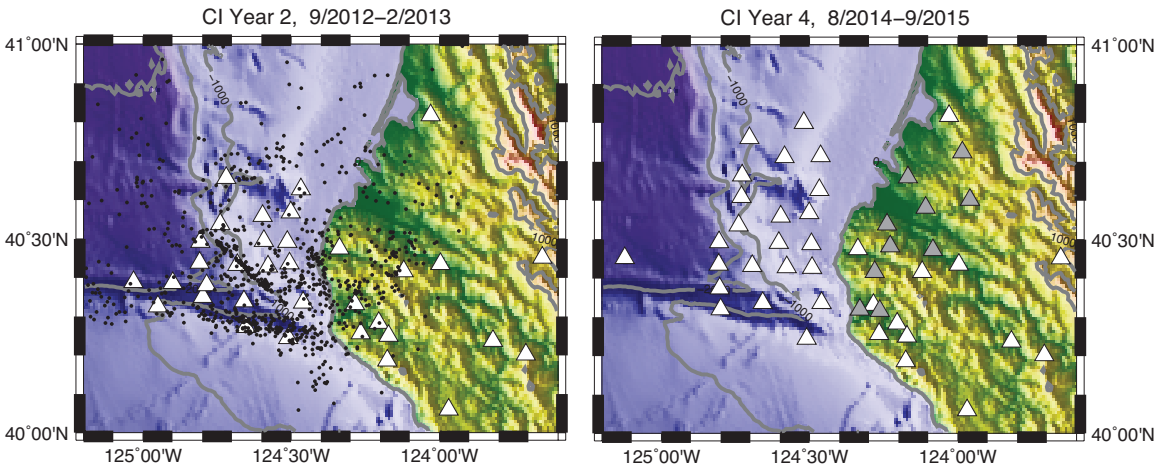

Figure 2. Cascadia Initiative Year 2 (left) and Year 4 (right) deployment maps. Black dots in the year 2 map denote seismicity relocated in the 3D velocity model. In the year 4 map, the white triangles onshore denote permanent stations (PBO+NCSN) and the gray triangles denote temporary PASSCAL instruments deployed by CIET (A. Trehu lead).

Relevance to USGS/EHP Priorities and Reducing Losses

Our proposed project is directly related to several Priority Topics for Research in the Pacific Northwest (PNA). In particular, in the 2016 announcement it specifically identifies the following topics:

- *Usage of the NSF-sponsored Cascadia initiative onshore-offshore deployments.*
- *Develop and test new approaches to integrating seismic and geodetic data and a priori information in monitoring operations, applicable to earthquake early warning, routine earthquake monitoring, tsunami warning, and slow slip detection and characterization.*
- *Provide local and regional information on shallow crustal structure (e.g., sedimentary basins) to improve the existing 3D seismic velocity models for Cascadia, with application to locating earthquakes, simulating ground motions, determining source mechanisms,…*
- *Improve estimates of fault-zone properties, such as degree of coupling and failure strength, that may influence rupture area and seismic slip on the Cascadia plate boundary.*

Our new 3D seismic velocity model of the most seismically active portion of the Cascadia Subduction zone helps with the above NEHRP goals. High-resolution seismic velocity models are necessary for real-time and routine catalog earthquake location, magnitude, and focal mechanism studies. In particular, the revised location of the thrust interface will be a key ingredient into ground motion predictions from large ruptures on it.

We have been working on the Cascadia Initiative data from the Mendocino Triple Junction (MTJ) region for a few years. Our basic cataloging and location work made it clear that the existing structural models in the region are not sufficient. The active source work in the 1990s was summarized by a highly complex 3D P-wave velocity model of Hole et al. [2000] that is shown in Figure 3. While this is likely a good first order 3D

model, it is still quite smooth and it does not address the spatial variations in the Vp/Vs ratio, which are significant.

To improve the velocity model, we use a combined database of first arrivals and waveform differential arrival times. It includes a number of data sources:

1. Our own picks and correlation times from both the Year 2 and Year 4 CI datasets including the onshore PASSCAL deployment.
2. The differential time measurement made in this region by Felix Waldhauser et al from roughly 2000 – present. The associated NCSN catalog times are also included.
3. We have picked a number of earthquakes that were recorded on Earthscope flex array and transportable array deployments in 2007-2009.

The tomographic imaging work is being done primarily by PhD Student Hao Guo. Hao is a fifth year student at USTC who is spending ~1 year at WHOI as a guest student. In collaboration with his adviser Haiching Zhang. He is collaborating with MIT-WHOI student Jianhua Gong who has a lot of experience with the CI OBS data and is working on validating the tomography model using converted phases (see below).

Hao Guo developed a new tomographic method called 'triple-difference tomography' that solves directly for the Vp/Vs ratio and is an extension of the more familiar double-difference tomography (tomoDD) method of Zhang and Thurber [*H Zhang and Thurber*, 2003; 2006] developed by his advisor. This is a great approach for dense datasets, and in particular for OBS data because the extra layer of differencing (subtracting the S-wave differential times from the P-wave ones) has the advantage that any unmodeled residuals due to OBS clock drift are naturally subtracted out from the data and do not enter into the Vp/Vs inversion. Currently the inversion for the MTJ region uses about 10,000 earthquakes and about 100 seismic stations (Figure 3). Figure 4 shows three cross sections through the resulting velocity models. The subducted crust is shown as a region of high Vp/Vs that roughly tracks the McCrory et al. [2012] plate interface model. In some regions the interface model appears to be a few km to deep and lies within the subducted crust. We are currently working on finishing up the resolution tests for the model and deciding wether LFE earthquakes from Plourde et al. can be picked well enough to help the inversion. We expect to submit a paper on the model by early summer.

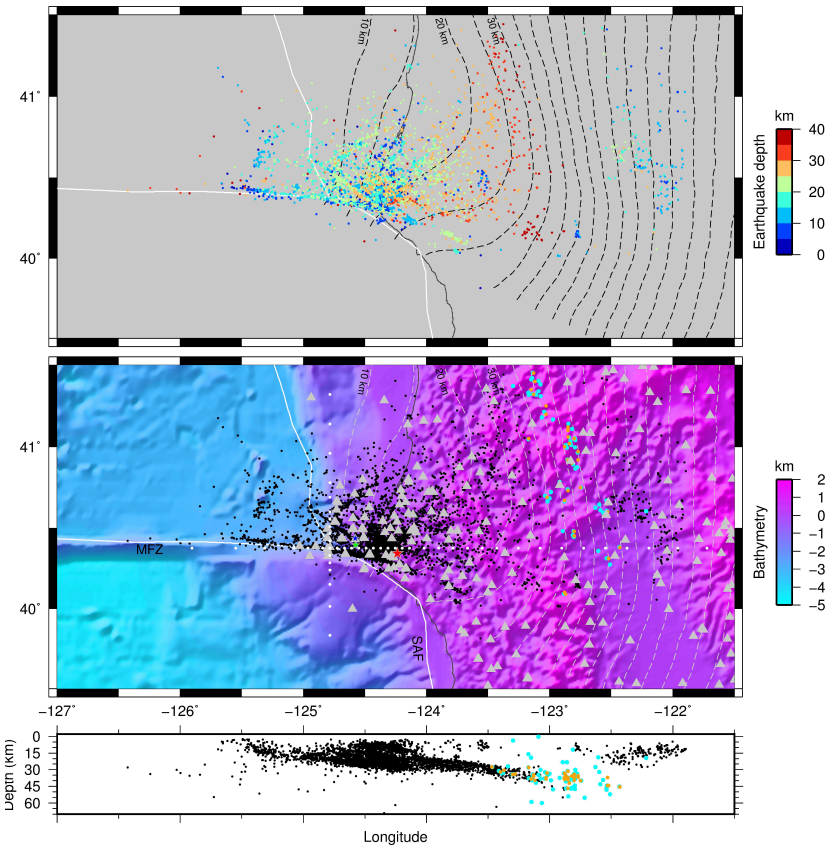

Figure 3. Relocated earthquake epicenters from the triple-difference (tomoDD) inversion. Slab contours are from McCrory et al., (2012). The white dots in the middle panel represent the x-y grid spacing for the tomographic inversion which is denseist in the region of the OBS network and shallow thrust interface. The lower panel shows a cross section through the region of active seismicity. The light blue and yellow circles denote the locations of individual LFES and LFE families from Plourde et al. (2015).

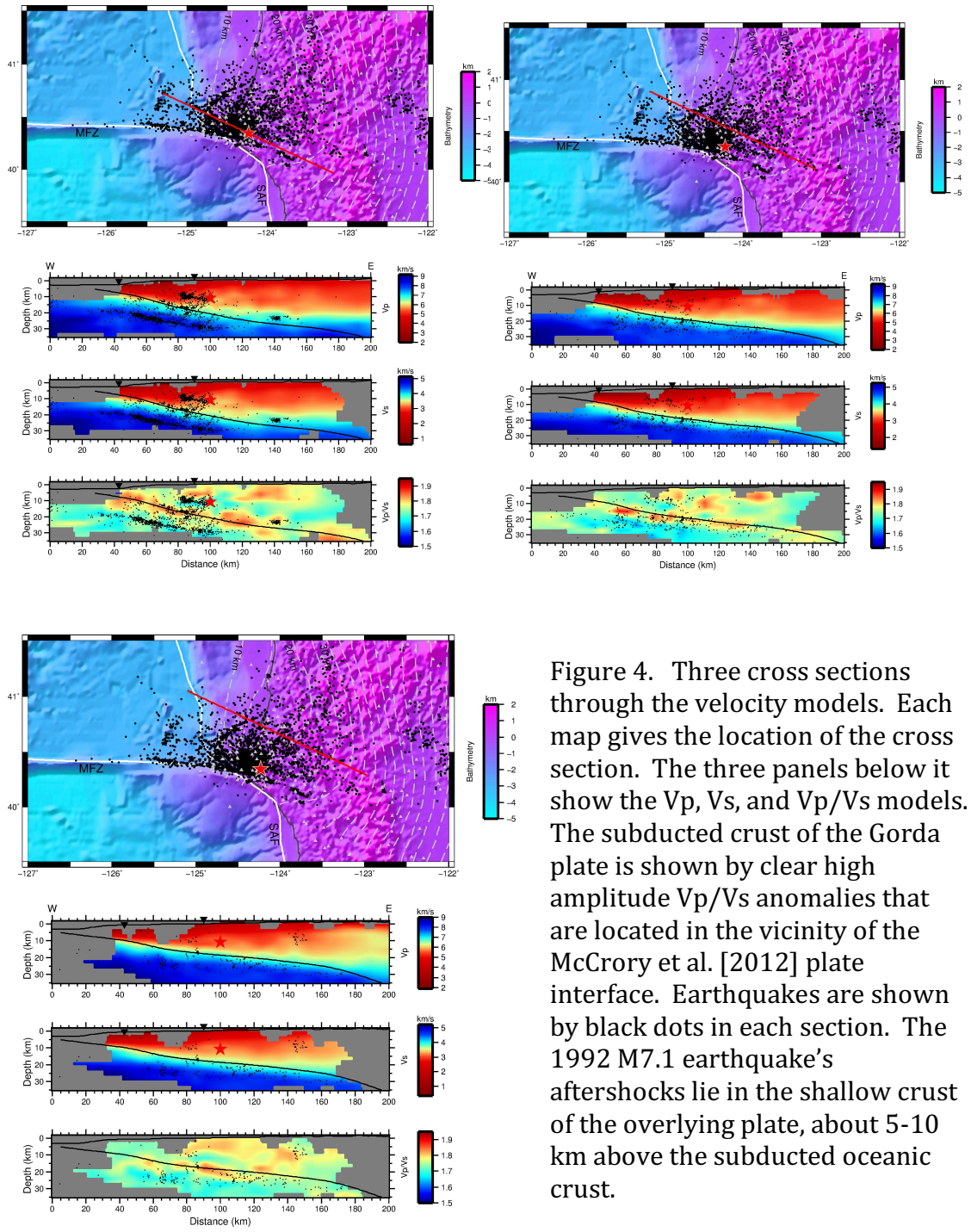

Figure 4. Three cross sections through the velocity models. Each map gives the location of the cross section. The three panels below it show the Vp, Vs, and Vp/Vs models. The subducted crust of the Gorda plate is shown by clear high amplitude Vp/Vs anomalies that are located in the vicinity of the McCrory et al. [2012] plate interface. Earthquakes are shown by black dots in each section. The 1992 M7.1 earthquake's aftershocks lie in the shallow crust of the overlying plate, about 5-10 km above the subducted oceanic crust.

To evaluate the tomography model and to refine the structural model of where the plate interface is located, we have begun to utilize seismic energy converted from earthquakes in the subducting Gorda plate that undergoes a conversion at the plate interface either from S-wave to P-wave or from P-wave to S-wave (Figure 5). Many such earthquakes show clear arrivals in between the direct P and S-waves, such as those seen on the vertical component of the records at station

B047 (Figure 6). These coherent arrivals, with a frequency around 5-10 Hz, show a moveout similar to the S-wave on the vertical component (for S-P), or similar to the P-wave on the horizontal component (for P to S) as would be expected from converted phases. Which is clearer varies from station to station. MIT-WHOI JP PhD student Jianhua Gong is currently evaluating both the velocity model and the interface model using the converted phase arrival times.

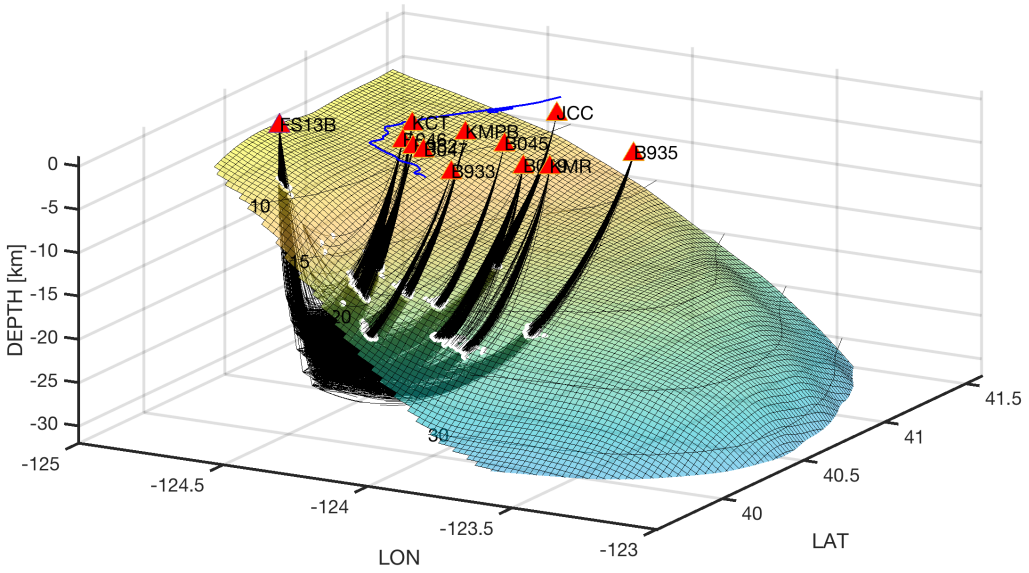

Figure 5. Ray paths from a cluster of earthquakes in the subducting Gorda plate to a number of onshore seismic stations and one offshore OBS. The colored surface is the slab interface model of McCrory et al. (2012).

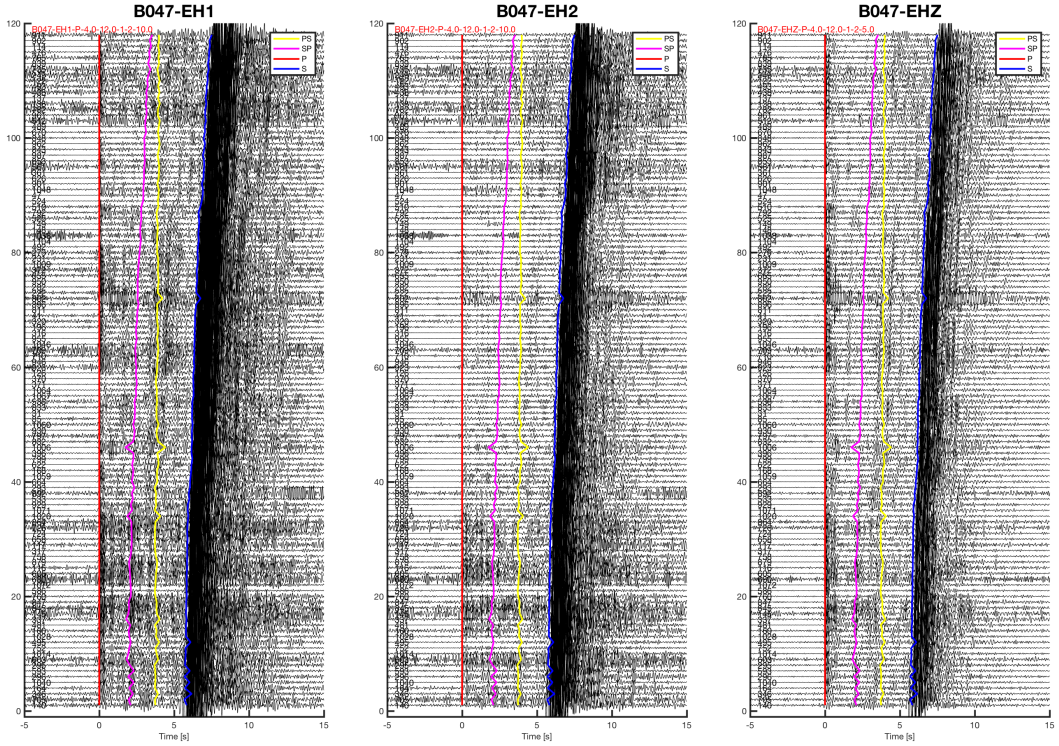

Figure 6. Waveform sections of the earthquakes in Figure 5 at the PBO borehole seismic station B047. Waveforms are sorted by travel time difference between P and S arrivals. Red, blue, yellow and pink lines are predicted P, S, Ps and Sp wave arrive times based on slab interface model from McCrory et al. (2012). All the seismograms are aligned on the P wave.

References.

Boyarko, D. C., and M. R. Brudzinski (2010), Spatial and temporal patterns of nonvolcanic tremor along the southern Cascadia subduction zone, *Journal of Geophysical Research: Solid Earth*, *115*(B8), B00A22.

Chen, X., and J. J. McGuire (2016), Measuring earthquake source parameters in the Mendocino Triple Junction region using a dense OBS array: implications for fault strength variations, *submitted to EPSL*.

Crawford, W. C., and S. C. Webb (2000), Identifying and removing tilt noise from low-frequency (< 0.1 Hz) seafloor vertical seismic data, *Bull. Seismol. Soc. Amer.*, *90*(4), 952-963.

Crawford, W. C., and S. C. Singh (2008), Sediment shear properties from seafloor compliance measurements: Faroes-Shetland basin case study, *Geophysical Prospecting*, *56*(3), 313-325.

Crawford, W. C., S. C. Webb, and J. A. Hildebrand (1991), SEA-FLOOR COMPLIANCE OBSERVED BY LONG-PERIOD PRESSURE AND DISPLACEMENT MEASUREMENTS, *J. Geophys. Res.-Solid Earth*, *96*(B10), 16151-16160.

Crawford, W. C., S. C. Webb, and J. A. Hildebrand (1999), Constraints on melt in the lower crust and Moho at the East Pacific Rise, 9 degrees 48 ' N, using seafloor compliance measurements, *J. Geophys. Res.-Solid Earth*, *104*(B2), 2923-2939.

Goldfinger, C., et al. (2012), Turbidite event history-Methods and implications for Holocene paleoseismicity of the Cascadia subduction zone, *U.S. Geol. Surv. Profess. Paper*, *1661-F*, 184.

Hole, J. A., B. C. Beaudoin, and S. L. Klemperer (2000), Vertical extent of the newborn San Andreas fault at the Mendocino triple junction, *Geology*, *28*(12), 1111-1114.

Llenos, A. L., and J. J. McGuire (2011), Detecting aseismic strain transients from seismicity data, *J. Geophys. Res.-Solid Earth*, *116*, 17.

McCrory, P. A., J. L. Blair, F. Waldhauser, D. H. Oppenheimer, (2012), Juan de Fuca slab geometry and its relation to WadatiBenioff zone seismicity, J. Geophys. Res., 117, doi:10.1029/2012JB009407.

McGuire, J. J., R. B. Lohman, R. D. Catchings, M. J. Rymer, and M. R. Goldman (2015), Relationships among seismic velocity, metamorphism, and seismic and aseismic fault slip in the Salton Sea Geothermal Field region, *Journal of Geophysical Research: Solid Earth*, *120*(4), 2014JB011579.

Murray, M. H., G. A. Marshall, M. Lisowski, and R. S. Stein (1996), The 1992 M=7 Cape Mendocino, California, earthquake: Coseismic deformation at the south end

of the Cascadia megathrust, *J. Geophys. Res.-Solid Earth*, *101*(B8), 17707-17725.

Plourde, A. P., M. G. Bostock, P. Audet, A. M. Thomas, (2015), Low-frequency earthquakes at the Southern Cascadia margin, Geophys. Res. Let., 42, doi:10.1002/2015GL064353.

Schmalzle, G. M., R. McCaffrey, and K. C. Creager (2014), Central Cascadia subduction zone creep, *Geochemistry, Geophysics, Geosystems*, *15*(4), 1515-1532.

Tanioka, Y., and T. Seno (2001), Sediment effect on tsunami generation of the 1896 Sanriku tsunami earthquake, *Geophys Res Lett*, *28*(17), 3389-3392.

Wei, M., and J. J. McGuire (2014), The Mw 6.5 offshore Northern California earthquake of 10 January 2010: Ordinary stress drop on a high-strength fault, *Geophys Res Lett*, 2014GL061043.

Williams, C. A., and L. M. Wallace (2015), Effects of material property variations on slip estimates for subduction interface slow-slip events, *Geophys Res Lett*, *42*(4), 1113-1121.

Yamamoto, T., M. V. Trevorrow, M. Badiey, and A. Turgut (1989), DETERMINATION OF THE SEABED POROSITY AND SHEAR MODULUS PROFILES USING A GRAVITY-WAVE INVERSION, *Geophys J Int*, *98*(1), 173-182.

Yuan, T., G. D. Spence, and R. D. Hyndman (1994), Seismic velocities and inferred porosities in the accretionary wedge sediments at the Cascadia margin, *J. Geophys. Res.,*, *99*, 4413-4427.

Zhang, H., and C. Thurber (2003), Double-difference tomography: The method and its application to the Hayward fault, California, *Bull. Seism. Soc. Am.*, *93*(5).

Zhang, H., and C. Thurber (2006), Development and Applications of Double-difference Seismic Tomography, *Pure and Applied Geophysics*, *163*(2), 373-403.

Zhang, H. J., C. H. Thurber, D. Shelly, S. Ide, G. C. Beroza, and A. Hasegawa (2004), High-resolution subducting-slab structure beneath northern Honshu, Japan, revealed by double-difference tomography, *Geology*, *32*(4), 361-364.